PHYSICAL REVIEW B

CONDENSED MATTER AND MATERIALS PHYSICS

THIRD SERIES, VOLUME 60, NUMBER 19 **15 NOVEMBER 1999-I**

BRIEF REPORTS

Brief Reports are accounts of completed research which, while meeting the usual **Physical Review B** *standards of scientific quality, do not warrant regular articles. A Brief Report may be no longer than four printed pages and must be accompanied by an abstract. The same publication schedule as for regular articles is followed, and page proofs are sent to authors.*

First-principles calculation of the effect of atomic disorder on the electronic structure of the half-metallic ferromagnet NiMnSb

D. Orgassa* and H. Fujiwara

Center for Materials for Information Technolgy (MINT), The University of Alabama, Tuscaloosa, Alabama 35487-0209

T. C. Schulthess and W. H. Butler

Oak Ridge National Laboratory, Oak Ridge, Tennessee 37831-6114

(Received 28 June 1999)

The electronic structure of the half-metallic ferromagnet NiMnSb with three different types of atomic disorder is calculated using the layer Korringa-Kohn-Rostoker method in conjunction with the coherent potential approximation. Results indicate the presence of minority-spin states at the Fermi energy for degrees of disorder as low as a few percent. The resulting spin polarization below 100% is discussed in the light of experimental difficulties confirming the half-metallic property of NiMnSb thin films directly. [S0163-1829(99)04743-8]

Half-metallic ferromagnets are ferromagnets with a minority- or majority-spin band gap at the Fermi energy. These materials are interesting because of possible applications in spin-polarized electronics[1] since the performance of spin-dependent devices like ferromagnetic tunnel junctions as well as spin valves generally improves if the conduction electrons are completely spin polarized. Half-metallic materials have been found in the transition metal oxides CrO_2 and Fe_3O_4 and in the colossal magnetoresistance material $La_{0.7}Sr_{0.3}MnO_3$. The first materials predicted to be half-metallic ferromagnets are the semi-Heusler compounds NiMnSb and PtMnSb which crystallize in the $C1_b$ structure.[2–6] While PtMnSb attracts much interest because of its large Kerr rotation,[7] NiMnSb is interesting because of its high Curie temperature of approximately 728 K.[8] NiMnSb and PtMnSb are very similar in many respects. This is strikingly demonstrated in magnetic measurements on Ni-substituted PtMnSb.[9]

Experimentally, the half-metallic property in bulk NiMnSb is reasonsably established. As expected for a half-metallic ferromagnet, the T^2 (spin-flip) contribution to the temperature dependence of the resistivity is absent at low temperatures.[10,11] The magnetic moment is measured as $4.0\mu_B$ per primitve unit cell,[12] which is in agreement with the integer moment expected for a half-metallic ferromagnet. Hanssen *et al.*[13] compared angular correlations of positron annihilation radiation with theoretical expectations and established the half-metallic character of the band structure.

Attempts have been made to show the half-metallic character of NiMnSb thin films in tunnel junctions[14,15] and spin valves.[16,17] The results of these experiments show effective spin polarizations well below 100%. Recently, Soulen *et al.*[18] measured the spin polarization of several materials using an Andreev-reflection method. Results indicate only a value of 58% for the spin polarization of a NiMnSb film deposited by co-evaporation. This compares to values between 42% and 46.5% for Fe, Ni, and Co, 78% for $La_{0.7}Sr_{0.3}MnO_3$, and 90% for CrO_2.

The reason for these experimental difficulties is not entirely clear. One constraint in preparing thin-film samples is that they cannot be arbitrarily annealed without changing the film structure. Thus, the degree of substitutional atomic disorder is expected to be higher in thin films than in bulk samples.

Neutron diffraction measurements on bulk NiMnSb (powder), indeed, estimate the atomic disorder to be well below 10%.[12] Whereas, x-ray diffraction measurements on PtMnSb thin films by Kautzky *et al.*[19] are consistent with a level of

TABLE I. Types of disorder considered in this report. The second column shows the sites with interchange of atoms (or vacancies). Occupancies of the four lattice sites are shown for the three types of disorder.

Disorder		Occupancies			
Type	Scheme	Site A	Site B	Site C	Site D
A-B	$A \leftrightarrow B$	$Ni_{1-x}Mn_x$	Ni_xMn_{1-x}		Sb
C	$AB \leftrightarrow C$	Ni_{1-x}	Mn_{1-x}	Ni_xMn_x	Sb
C'	$BD \leftrightarrow C$	Ni	Mn_{1-x}	Mn_xSb_x	Sb_{1-x}

atomic disorder of approximately 10%. Kautzky and coworkers also measured a similar degree of disorder for NiMnSb.[20] It has been pointed out that atomic disorder has a strong influence on the half-metallic property of PtMnSb.[4]

In this paper, we apply the layer Korringa-Kohn-Rostoker method[21] in conjunction with the coherent potential approximation (LKKR-CPA) to study the electronic structure of NiMnSb with three different types of disorder.

The crystal structure of the NiMnSb compound is $C1_b$. This structure consists of four interpenetrating fcc sublattices equally spaced along the [111] direction. The lattice sites A at 000, B at $\frac{1}{4}\frac{1}{4}\frac{1}{4}$, and D at $\frac{3}{4}\frac{3}{4}\frac{3}{4}$ are occupied by Ni, Mn, and Sb, respectively. The site C at $\frac{1}{2}\frac{1}{2}\frac{1}{2}$ is unoccupied in the ordered alloy. We use the atomic sphere approximation (ASA) with an empty sphere occupying site C in the perfect crystal. The experimental lattice constant[8] of 5.927 Å is used throughout. For the LKKR-CPA calculations we use the layer doubling algorithm,[21] repeating (110) layers with four sites in the layer unit cell. All numerical results are based on fully self-consistent calculations performed with a basis set that includes s, p, d, and f partial waves on each site and 75 two-dimensional plane waves. The Brillouin zone sums were performed over 64 special $\vec{k}_\parallel$ points in the Brillouin zone and for the energy integrals we used 16 points on a semicircle in the complex plane.

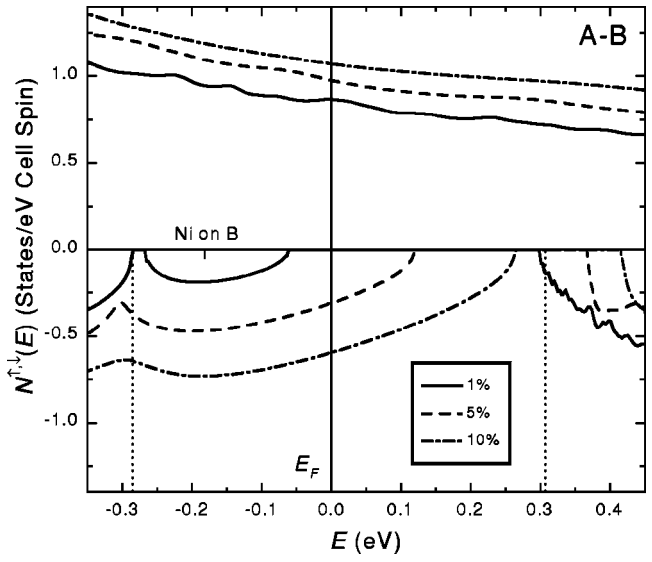

FIG. 1. Calculated spin-polarized electronic density of states $N^{\uparrow,\downarrow}(E)$ for NiMnSb with A-B-type disorder. Disorder levels x (see Table I) are 1% (solid lines), 5% (dashed lines), and 10% (dash-dotted lines). Minority-spin densities of states $N^{\downarrow}$ are plotted with a negative sign. The position of the minority-spin band gap in ordered NiMnSb is indicated by two dotted vertical lines. The position of disorder-induced minority-spin states, generated at low levels of disorder, is indicated by a mark on the energy axis.

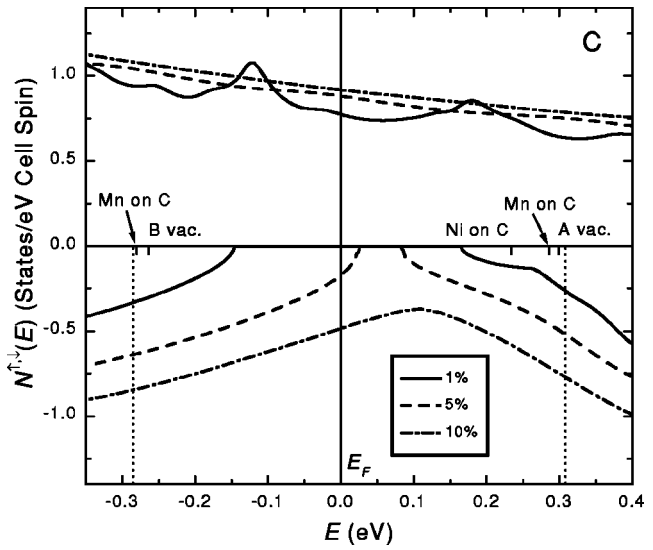

FIG. 2. Calculated spin-polarized electronic density of states $N^{\uparrow,\downarrow}(E)$ for NiMnSb with C-type disorder (see caption of Fig. 1 for further explanations).

We consider disorder by interchange of Ni and Mn as well as two types of disorder with a partially occupied C site. In all cases we retain the stoichimetric concentration. The three types of disorder are shown in Table I. Disorder of type A-B has an interchange of Ni and Mn atoms between the A and B sites. Type C has equal amounts of Ni and Mn atoms on the normally vacant lattice site C. In the case of type C', Mn and Sb atoms partially occupy site C. The x-ray diffraction measurements on NiMnSb thin films by Kautzky *et al.*[20] are consistent with C'-type disorder and a disorder level of $x = 5\%$.

The densities of states for all three types of disorder show

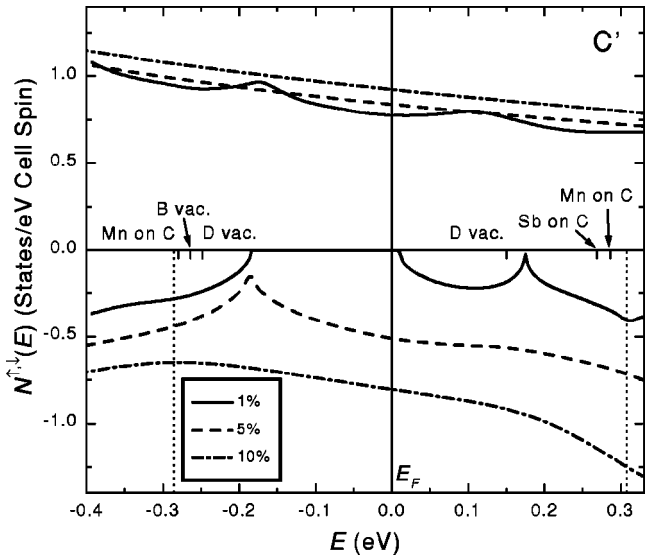

FIG. 3. Calculated spin-polarized electronic density of states $N^{\uparrow,\downarrow}(E)$ for NiMnSb with C'-type disorder (see caption of Fig. 1 for further explanations).

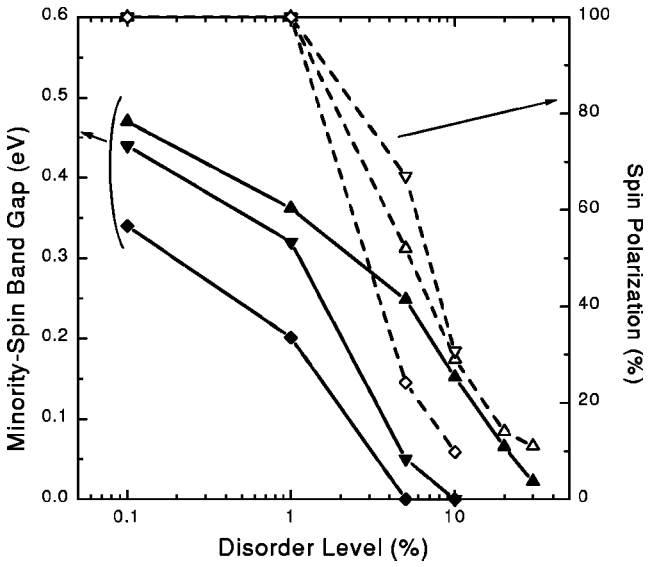

FIG. 4. Minority-spin band gap (solid symbols and lines) and spin polarization at the Fermi energy (open symbols and dashed lines) as a function of the disorder level for *A*-*B*-type disorder (up triangles), *C*-type disorder (down triangles), and *C′*-type disorder (diamonds). The lines between the data points are to guide the eyes.

additional minority-spin states in the energy range of the band gap of the ordered material. These states widen with increasing disorder. This behavior leads to a reduced minority-spin band gap and a displacement of the Fermi energy relative to the original band gap. In all three cases, this causes a reduced spin polarization for higher levels of disorder. In order to understand the nature of the disorder-induced minority-spin states, we perform calculations for only 0.01% occupancy of a single kind of atom (or vacancy) on another lattice site. The results allow us to assign a certain impurity to each disorder-induced state.

Figure 1 shows the electronic densities of states for *A*-*B*-type disorder with disorder levels of 1%, 5%, and 10%. For low levels of disorder, additional states at approximately 0.10 eV above the bottom of the minority-spin band gap are present. These states are generated by the presence of Ni at site *B*. The energy range of these states widens with increasing disorder and, from between 1% and 5% on, includes the Fermi energy.

The density of states for *C*-type disorder at disorder levels of 1%, 5%, and 10% is shown in Fig. 2. Here, all four impurity atoms (or vacancies) contribute additional minority-spin states. For low levels of disorder there are separate states for Ni on site *C* ($\approx$0.07 eV below the top of the gap), for Mn on site *C* ($\approx$0.02 below the top of the gap), for vacancies on site *A* ($\approx$0.01 eV below top of the gap), and for vacancies on site *B* ($\approx$0.02 eV above the bottom of the gap). As in the previous case, a 5% disorder is sufficient to generate minority-spin states at the Fermi energy.

Figure 3 shows the density of states for 1%, 5%, and 10% disorder of the *C′* type. As in the previous case, impurity states due to Mn on site *C* and vacancies on site *B* appear for low levels of disorder. The presence of Sb on site *C* causes states at approximately 0.04 eV below the top of the gap, while the vacancies on site *D* generate states at approximately 0.04 eV above the bottom of the gap and approximately 0.16 eV below the top of the gap. As in the other two cases, the energy ranges of these states widen with increasing disorder. Just above a disorder level of 1% these states reach the Fermi energy and reduce the spin polarization.

TABLE II. Total spin polarization *P* and *s*-electron spin polarization P_s for disordered NiMnSb.

Type	Disorder Level (%)	*P* (%)	P_s (%)
A-*B*	5	52	82
	10	29	64
C	5	67	89
	10	31	60
C′	5	24	34
	10	10	19

The spin polarization at the Fermi energy *P* is defined as

$$P=\frac{N^{\uparrow}(E_F)-N^{\downarrow}(E_F)}{N^{\uparrow}(E_F)+N^{\downarrow}(E_F)}, \tag{1}$$

where $N^{\uparrow,\downarrow}$ is the spin-up (spin-down) density of states and E_F is the Fermi energy. The calculated spin polarization *P* as well as the minority-spin band gap are summarized in Fig. 4. One can see that any of the considered disorder modes is capable of significantly reducing the spin polarization at disorder levels of as low as a few percent. For the experimentally observed *C′* disorder with a disorder level of 5%, we find a low spin polarization of 24% and a vanishing minority-spin band gap.

Tunneling experiments generally do not measure the spin polarization *P* at the Fermi energy. In these experiments the tunneling current usually is dominated by *s*-type electrons. Table II shows the calculated spin polarizations *P* and compares these with the spin polarizations due to the *s* electrons P_s, defined as

$$P_s=\frac{N_s^{\uparrow}(E_F)-N_s^{\downarrow}(E_F)}{N_s^{\uparrow}(E_F)+N_s^{\downarrow}(E_F)}, \tag{2}$$

where $N_s^{\uparrow,\downarrow}$ is the *s* electron density of states. Although P_s is always larger than *P* for a given disorder, it follows the same trend with increasing disorder.

In conclusion, we have shown that atomic disorder in NiMnSb at a level experimentally observed in thin films leads to minority-spin states at the Fermi energy and a reduction of the spin polarization. We want to point out that surface segregation and the electronic structure at the interfaces will influence measured spin polarizations as well. We expect that more data on disorder in thin-film samples as well as spin-polarization measurements on surfaces of bulk samples as a function of annealing parameters will be helpful in clarifying the reason for the low experimental spin polarizations in NiMnSb thin films.

This work has been supported by the United States Department of Energy, Office of Basic Energy Sciences through Contract No. DE-AC05-96OR22464 with Lockheed Martin Energy Research, Inc. and the U.S. Department of Defense under Grant No. DAAH04-96-1-0316.

*Electronic address: dorgassa@mint.ua.edu

[1] G. Prinz, Phys. Today **48** (4), 58 (1995).
[2] R. A. de Groot, F. M. Mueller, P. G. van Engen, and K. H. J. Buschow, Phys. Rev. Lett. **50**, 2024 (1983).
[3] E. Kulatov and I. I. Mazin, J. Phys.: Condens. Matter **2**, 343 (1990).
[4] H. Ebert and G. Schütz, J. Appl. Phys. **69**, 4627 (1991).
[5] Xindong Wang, V. P. Antropov, and B. N. Harmon, IEEE Trans. Magn. **30**, 4458 (1994).
[6] S. J. Youn and B. I. Min, Phys. Rev. B **51**, 10 436 (1995).
[7] P. G. van Engen, K. H. J. Buschow, and R. Jongebreur, Appl. Phys. Lett. **42**, 202 (1983).
[8] M. J. Otto *et al.*, J. Phys.: Condens. Matter **1**, 2341 (1989).
[9] P. P. J. van Engelen, D. B. de Mooij, J. H. Wijngaard, and K. H. J. Buschow, J. Magn. Magn. Mater. **130**, 247 (1994).
[10] M. J. Otto *et al.*, J. Phys.: Condens. Matter **1**, 2351 (1989).
[11] J. S. Moodera and D. M. Mootoo, J. Appl. Phys. **76**, 6101 (1994).
[12] R. B. Helmholdt *et al.*, J. Magn. Magn. Mater. **43**, 249 (1984).
[13] K. E. H. M. Hanssen, P. E. Mijnarends, L. P. L. M. Rabou, and K. H. J. Buschow, Phys. Rev. B **42**, 1533 (1990).
[14] R. Kabani, M. Terada, A. Roshko, and J. S. Moodera, J. Appl. Phys. **67**, 4898 (1990).
[15] C. T. Tanaka, J. Nowak, and J. S. Moodera, J. Appl. Phys. **81**, 5515 (1997).
[16] C. Hordequin, J.P. Nozières, and J. Pierre, J. Magn. Magn. Mater. **183**, 225 (1998).
[17] J. A. Caballero *et al.*, J. Vac. Sci. Technol. A **16**, 1801 (1998).
[18] R. J. Soulen, Jr. *et al.*, Science **282**, 85 (1998).
[19] M. C. Kautzky *et al.*, J. Appl. Phys. **81**, 4026 (1997).
[20] M. C. Kautzky *et al.* (unpublished).
[21] J. M. MacLaren, S. Crampin, D. D. Vvedensky, and J. B. Pendry, Phys. Rev. B **40**, 12 164 (1989).